

# Evaluating uncertainties in satellite altimeter sea state data via triple collocation during the Jason-3/Sentinel-6MF Tandem Experiment

Ben Timmermans <sup>1,\*</sup> , Christine P. Gommenginger <sup>1</sup>  and Craig J. Donlon <sup>2</sup>

<sup>1</sup> National Oceanography Centre, Southampton, SO14 3ZH, United Kingdom

<sup>2</sup> European Space Agency ESA/ESTEC, Keplerlaan 1, 2201, AZ, Noordwijk, the Netherlands

\* Corresponding author: ben.timmermans@gmail.com, cg1@noc.ac.uk

**Abstract:** The growing satellite record of sea state observations is becoming increasingly important for climate change research, to improve ocean and weather forecasts and to inform climate change mitigation and investment strategies. The Copernicus Sentinel-6 Michael Freilich (S6-MF) mission was launched in November 2020 by the European Space Agency to succeed Jason-3 (J3) as the long term satellite altimetry reference mission. S6-MF commissioning involved a unique 12 months Tandem Experiment during which S6-MF flew approximately 30 seconds behind J3 on the same ground tracks, resulting in an unprecedented global dataset of quasi-simultaneous collocated altimeter sea state measurements in Low-Resolution Mode (LRM) and Synthetic Aperture Radar (SAR) mode. In this work, this unique dataset is examined to evaluate uncertainties in altimeter significant wave height (Hs) observations from the two missions in different operating modes and different sea state conditions. S6-MF and J3 data are compared with *in situ* buoy measurements and reanalysis data using, amongst other methods, triple collocation analysis. Results indicate that, over the global ocean, J3 and S6-MF Low-Resolution Hs show almost perfect agreement, with near-zero mean bias and RMSE of XXX. In contrast, S6-MF SAR With respect to J3, Hs measurements from S6-MF scanning aperture radar (SAR) were found to suffer from high bias and increased random error. Error calculations from the triple collocation were found to be \*\*\* sensitivity \*\*\* with respect to oceanic region / sea state / swell buoy type / direction of overpass. However, subsampling of the overall global datasets, and the subsequent reduction in collocated dataset, led to considerable reduction in confidence for some analyses. These findings demonstrates the value of such a unique experimental configuration.

**Keywords:** Global sea state; satellite altimetry; sentinel-6 tandem; triple collocation; significant wave height

**Citation:** Timmermans, B., C. Gommenginger and C. J. Donlon  
Uncertainties in satellite altimeter sea state via triple collocation during the Jason-3/Sentinel-6MF Tandem Experiment. *Remote Sens.* **2022**, *1*, 0.  
<https://doi.org/>

Received:

Accepted:

Published:

**Publisher's Note:** MDPI stays neutral with regard to jurisdictional claims in published maps and institutional affiliations.

**Copyright:** © 2022 by the authors. Submitted to *Remote Sens.* for possible open access publication under the terms and conditions of the Creative Commons Attribution (CC BY) license (<https://creativecommons.org/licenses/by/4.0/>).

## 1. Introduction

Studies of ocean surface wave variability and trends are relevant to many scientific questions and marine applications. Historically, such research relied almost exclusively on numerical hindcast or reanalysis datasets, owing to the general lack of global sea state observations. However, sea state reanalysis products suffer specific deficiencies in this long-term context [1,2], and even *in situ* observations from wave buoys - the 'gold standard' used routinely to calibrate and validate models and satellites - are known to introduce problems when considering longer time scales [3,4]. Satellite remote sensing now offers global observations of multiple sea state parameters that are often exploited in tandem with numerical simulations, or can be used separately, as an independent source of historical sea state information. Sea state observations from satellites are increasing in duration, abundance, variety and applications. For example, the European Space Agency Sea State Climate Change Initiative (CCI) has set out to produce Climate Data Records (CDR) of Essential Climate Variables (ECV) for Sea State using carefully cross-calibrated data from multiple satellites flown since 1992 [5]. Recent studies that exploit the Sea State CCI

products include the evaluation of sea state conditions near the coast [6], estimations of global wave power [7], the examination of sea state and ocean current interactions [8] and studies of long term sea state variability [9,10]. The continuity of, and our ability to maintain, high quality remotely sensed sea state information is therefore more important than ever.

The European Space Agency's Sentinel-6 Michael Freilich (S6-MF) mission, launched in 2020, succeeded Jason-3 (J3) as the long term altimetry reference mission in April 2022. S6-MF commissioning involved a somewhat unique 18 month duration tandem phase experiment (S6-JTEX) such that S6-MF followed J3 in the same orbit, lagging by approximately 30 seconds, providing the opportunity to generate a substantial record of closely collocated altimetry measurements of sea surface significant wave height (Hs) from these two missions. J3, launched in 2016, obtains measurements of surface significant wave height from the onboard Poseidon 3B altimeter in low resolution mode (LRM). Similarly, S6-MF carries a Poseidon 4B altimeter that can also acquire measurements of Hs in low resolution mode. However, the Poseidon 4B instrument is a nadir-pointing dual-frequency synthetic aperture radar (SAR) altimeter designed to provide high accuracy and high precision altimetry measurements. As such, measurements of Hs are made in both LRM and SAR modes providing a valuable opportunity to assess their respective performances and, for the first time, to evaluate the performance of the new S6-MF SAR Interleaved mode (Gommenginger et al., 2013) directly against S6-MF LRM and J3 (LRM). The S6-MF/Jason-3 Tandem will provide the opportunity to explore the relative merits of difference modes and satellites (biases, random errors, continuity) in different oceanic conditions (e.g. high waves, swell, low winds).

In this work we exploit this unique experimental configuration to examine uncertainties in wave height observations from altimetry from the two missions in the tandem phase, together with a range of other high quality long term sea state datasets, from both *in situ* measurements and reanalysis. This study uses triple collocation as the central methodology to assess data from S6-MF and J3, different S6-MF operating modes, independent *in situ* fiducial data and global models. Triple collocation is a powerful statistical tool that makes it possible to quantify measurement uncertainties in three independent datasets, without assumptions about the quality of either data source. This study follows a similar, but shorter, earlier experiment with Sentinel-3A and -3B that established the viability of such a configuration for collocation studies. However, the 6-months tandem phase for Sentinel-3A/B resulted in a relatively small number of collocations with buoys suggesting that the triple collocation analyses would have benefitted (for the sake of robustness) from a longer tandem period. The longer XX-month tandem phase therefore allows for greater robustness in results.

In this paper, we describe and evaluate uncertainties in the S6-MF and J3 tandem Hs data. In Section 2 we describe the methods and datasets, including the triple collocation approach. Results are presented in Section 3, firstly examining global summaries from a range of datasets, and then exploring the sensitivity of these results to \*\*\* geographic location, nearshore and offshore regions, and finally sea state and swell. In Section 4, we discuss these results and the implications for the long term sea state record.

## 2. Data and Methods

In this section, we describe the Hs observation obtained from S6-MF and J3, and other sea state datasets used in the paper, and the statistical tools and methods used to evaluate the uncertainties across these different datasets.

### 2.1. Satellite altimeter products: Jason-3 LRM, Sentinel-6 LRM and SAR

Altimeter data from all instruments was obtained for the complete tandem phase beginning December 2020 until April 2022. The Jason-3 Geophysical Data Record processing baseline F v1.01 [J3 product handbook] provides along track 1 Hz observations of significant wave height processed from the onboard Poseidon-3B altimeter. In this paper we use

primarily the Ku band corrected significant wave height *swh\_ocean*, together with quality control indication from *swh\_ocean\_compression\_quality*, *swh\_ocean\_compression\_quality* and *swh\_ocean\_numval*. Additional sensitivity studies are provided with respect to the "MLE3" retracking. \*\*\* TBD

Processed from the Poseidon-4B altimeter onboard S6 [S6 refs \*\*\*], along track "Non-Time Critical" (NTC) 1 Hz observations of significant wave height from Sentinel-6 LRM and SAR are provided in the F06 baseline processing from EUMETSAT. As for *ocean\_swh* is computed from the ocean retracker including all instrumental corrections. Quality control indicators follow the convention of Jason-3, with the same variable names provided. Note that only a single retracking method ("ocean retracker") is available.

## 2.2. Satellite altimeter quality control

\*\*\* Quality control criteria TBD and subject to change.

Outliers can have a substantial impact on the results of a triple collocation analysis so it important to appropriately account for spurious data in the altimetry record. Choice of quality control and error identification. Issues with differences between J3 and S6 error flagging (quality / 20Hz numval / 20Hz sd) \*\*\*

## 2.3. In situ wave platforms

A substantial, if not vast, majority of studies of sea state variability over recent decades have relied critically upon a multitude of *in situ* platforms that have been deployed in the global oceans, in order to gather information about the sea state. These platforms are often operated by national agencies, leading to a diversity of different operating procedures that make the collection, analysis and intercomparison of the recorded measurements challenging. The largest proportion of these measurement stations, operated by the U.S National Data Buoy Center (NDBC) are routinely used as a reference. However, it is well known [3] that owing to operational changes through the years, and indeed lacking the specific objective to provide a stable and continuous long term record, that inconsistencies and data stability are problematic for long term analyses. In light of growing research interest in the long term sea state record and concerns raised by the the scientific community, researchers at the United State Army Corps of Engineers have recently performed a comprehensive re-evaluation and quality check of the entire NDBC record [11].

An alternative resource that attempts to overcome the challenges associated with data acquisition from the diversity of operational *in situ* platforms is the INSTAC, a component of the European Copernicus Marine Environment Monitoring Service (CMEMS). \*\*\* TBD

## 2.4. ERA5 reanalysis

ERA5 [12] is the most recent release of the well-know and widely used reanalysis products developed and distributed by ECMWF. Replacing the previous successful ERA40 and ERA Interim reanalyses, ERA5 provides global hourly analyses on a 50 km grid of numerous parameters of the atmosphere, land surface, ocean and ocean waves from 1950 to present. Compared to its predecessors, ERA5 introduced a number of innovations, notably with hourly assimilation of satellite altimeter significant wave height data. At the time of writing, ERA5 assimilates altimeter Hs data from a number of altimeter missions but importantly with the exception of J3 [13]. In this study, comparative analyses use the ERA5 hourly mean products for Hs, average wave period and swell Hs (first partition). \*\*\*

## 2.5. ESA Sea State CCI SAR Wave Mode Level 2 products

SAR imagers operating in Wave Mode (WV) generate small images of the ocean surface approximately 20 km × 20 km called imaggettes (or vignettes) acquired at regular intervals along the orbit (typically every 100 km). The standard operational sea state outputs for Sentinel-1 are the Level 2 Ocean Swell Wave (OSW) products that contain two-dimensional ocean surface swell spectra derived from the co- and cross-spectra of the SAR images. In Wave Mode, one imaggette produces one directional swell spectrum. Integral wave

parameters can be derived from the directional spectrum, such as the significant swell height, dominant period and dominant direction of up to 5 swell partitions [14]. Other retrieval algorithms, such as C-WAVE [15], propose instead to extract wave parameters, such as significant wave height and wave periods, based on empirical relationships. Algorithms evolved from this approach have been implemented for Envisat ASAR [16] and for Sentinel-1 Interferometric Wide Swath Mode (IW) in near real-time processing services for maritime situational awareness [17]. Further developments specifically for Sentinel-1 WV historical data have also recently been completed [18]. This paper utilises SAR WV data in the CCI products obtained with the C-WAVE approach.

## 2.6. Drifting buoys

\*\*\* TBD

## 2.7. Error estimation using triple collocation method

The triple collocation method is a powerful means of estimating the random error of observations where three simultaneous observations of the same quantity can be made. Numerous examples of its application to geophysical variables such as wind speed and wave height can be found in the literature [19–21]. A detailed exposition of the method is provided by [22] who, in particular, identify several key assumptions:

1. Linear calibration is sufficient over the whole range of measurement values;
2. The reference measurement values are unbiased and calibrated;
3. The random measurement errors have constant variance over the whole range of calibrated measurement values;
4. The measurement errors are uncorrelated with each other (except for representation errors);
5. The random measurement errors are uncorrelated with the geophysical signal.

In reality, it may be difficult to satisfy all of these rigorously, point (4) being particularly challenging in the context of sea state since many datasets are inherently dependent upon the limited number of in situ measurements (see e.g. [19,23]). Reanalysis data is also strongly influenced by assimilation of altimetry observations, thus one might anticipate some level of error dependence, which is not easy to resolve.

### 2.7.1. Data Processing

\*\*\* TBD

Require detailed explanation of data processing:

- Buoy quality control: clearly a major issue (see [11] for NDBC) but also required for CMEMS TAC (e.g. [23])
- Satellite quality control: J3 vs S6 quality flagging, numval / sigma etc.
- Satellite sampling: required at scales appropriate to the geographic location and collocated data, without reducing overall sampling density and robustness of results (where possible)
- Spatial scale conformity and removal of representativity errors (see e.g. [22]). Might require sensitivity analysis.
- Time series smoothing and autocorrelation checking (moving average?).

### 2.7.2. Evaluation of error dependence in S6-JTEX data.

\*\*\* TBD

Not currently entirely clear how we can achieve this but it would highly advantageous in order to exploit a much larger dataset (and avoid using moored / drifting buoys). Perhaps J6-MF SAR is more useful in this context? Possible approach may involve steadily "whitening" altimetry data to establish relationship between all variables (possibly in regions covered by moored buoys)? Synthetic tests probably required.

### 3. Results

#### 3.1. Summary of tandem data

Summary data showing the global counts of track median samples from J3 during the tandem phase are shown in Figure 1. This reveals the characteristic chequered sampling pattern associated with altimeter orbits. The number of observations in adjacent cells near the equator can differ by a factor of  $\sim 2$ . At mid and high latitudes, as the separation between ground-tracks decreases, this effect is much less pronounced. Very little variation in this sampling structure can be seen between different years.

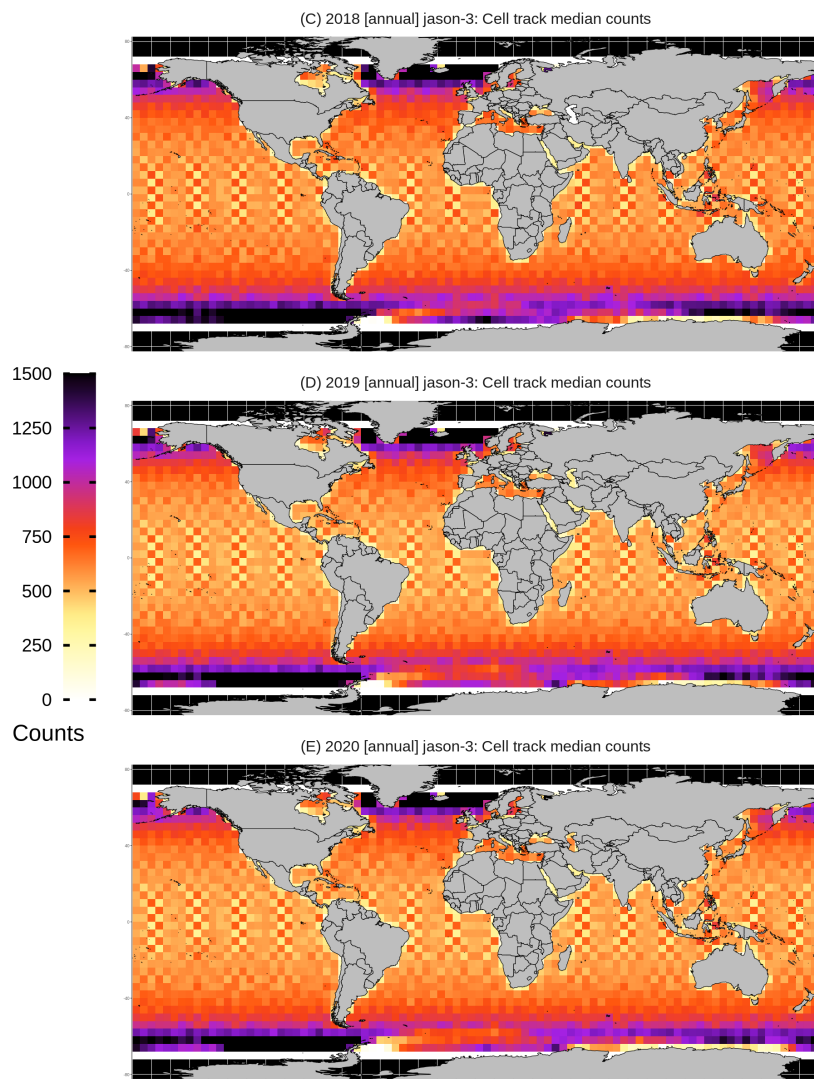


**Figure 1.** Annual counts of Jason-3 altimetry observations in 2018, 2019 and 2020 within  $4 \times 4$  degree grid cells over the global ocean. For this analysis, median values of 1Hz Hs measurements are used from each overpass. Note the heterogeneity between neighbouring cells in equatorial regions due to the orbital sampling and large track-to-track separation for Jason-3 at the Equator.

Properties of the collocated S6-JTEX data, together with moored buoys in the Pacific Ocean, are shown using scatterplot projections for pairwise comparisons. S6-JTEX data are collocated with hourly buoy data at the moored wave buoys from the U.S. National Data Buoy Center (NDBC, <https://www.ndbc.noaa.gov>) indicated in Figure 2. All chosen buoys pass quality control criteria (\*\*\*) TBD). Buoys designated as "offshore" satisfy a distance to coast criteria \*\*\* and are marked in yellow. Buoys designated as "nearshore" lie within \*\*\* criteria of the coast. Separation of sites based upon coastal proximity provides a means of

avoiding increased variability due to coastal effects. For example, sea state variability is  
anticipated to be subject to strong spatial gradients at many coastal locations \*\*\*. TBD.

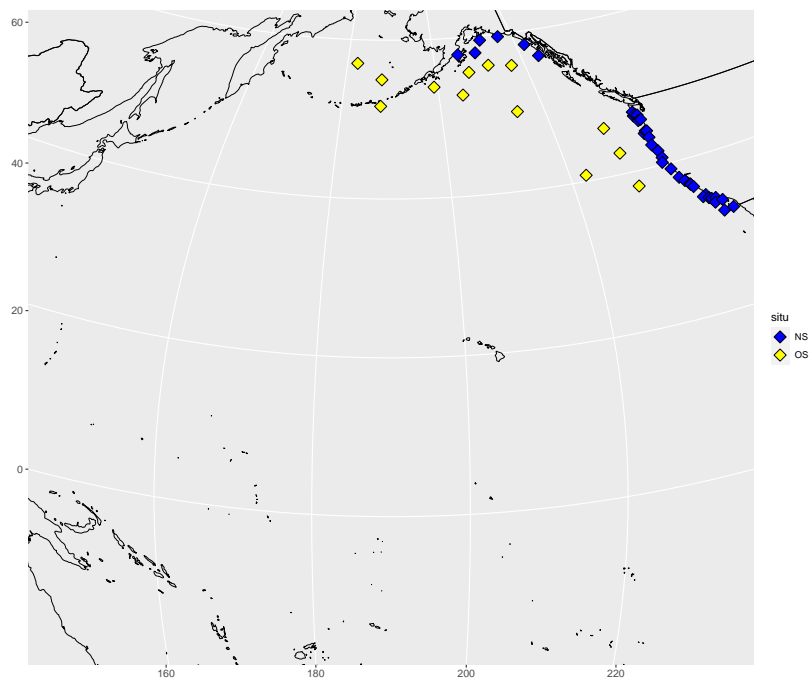


**Figure 2.** Locations of selected NDBC wave buoys used to collocate S6-JTEX data with *in situ* measurements of total Hs.



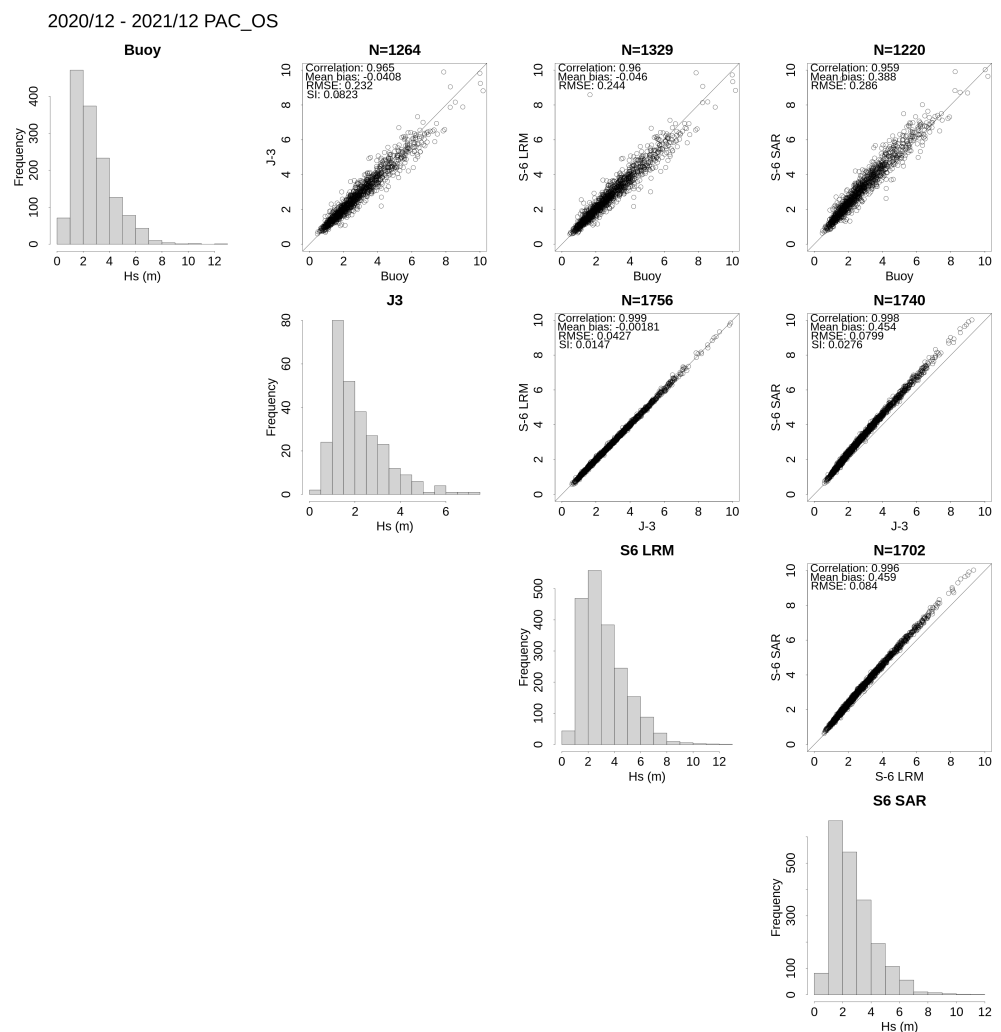


**Figure 3.** Collocations at Pacific offshore locations with 150 km sampling.

Figure 3 shows scatterplot projections of the possible pairwise comparisons of collocated data in the North Pacific offshore moored buoy locations shown in Figure 2. The relationships between the datasets are readily apparent and exhibit a number of distinct characteristics that are likely to manifest in the TC analysis. Starting with the comparisons with in situ buoys on the top row, there is noticeable scatter and RMSE, between 0.23 and 0.29 m, that is much larger than any of the other comparisons. This is likely linked, at least in part, to representativity error, since the altimeter tracks do not pass perfectly over mooring locations. Nonetheless, comparisons with the observations from the LRM instruments reveal low bias throughout the observed range of Hs. Of note, however, is the high mean bias (0.39 m) associated with the S6-MF SAR measurements (known problem \*\*\* TBD). Note also that numbers of collocations, shown at the top of each panel, vary a little owing to missing data in the constituent datasets.

Considering the intercomparisons with J3 (second row from top), the near zero bias, scatter of approximately 0.04 m and linear correlation of 1.0, characterise the remarkable agreement. No noticeable deviation in these properties is seen even at high values of Hs. Encouragingly, this finding suggests that, in terms of Hs observations, S6-MF will provide excellent continuity as the reference mission going forward, however, it raises questions as to the likelihood of dependence in observation errors which has important consequences for the application of the TC method. These are discussed further in Section \*\*\*. Note the considerably higher number of collocations (N=1756) follows from the good continuity of the altimetry acquisition, as opposed to the in situ buoys (N=1264) that can suffer periodic

outage. The intercomparison of J3 and S6-MF SAR exhibits a similar high mean bias (0.45 m). However, the high correlation and low RMSE clearly reveal the systematic nature of the bias, that appears to decrease somewhat at higher values. Finally, the intercomparison between S6-MF LRM and SAR acquisitions follows closely the intercomparison with J3, since the two correspond so closely.

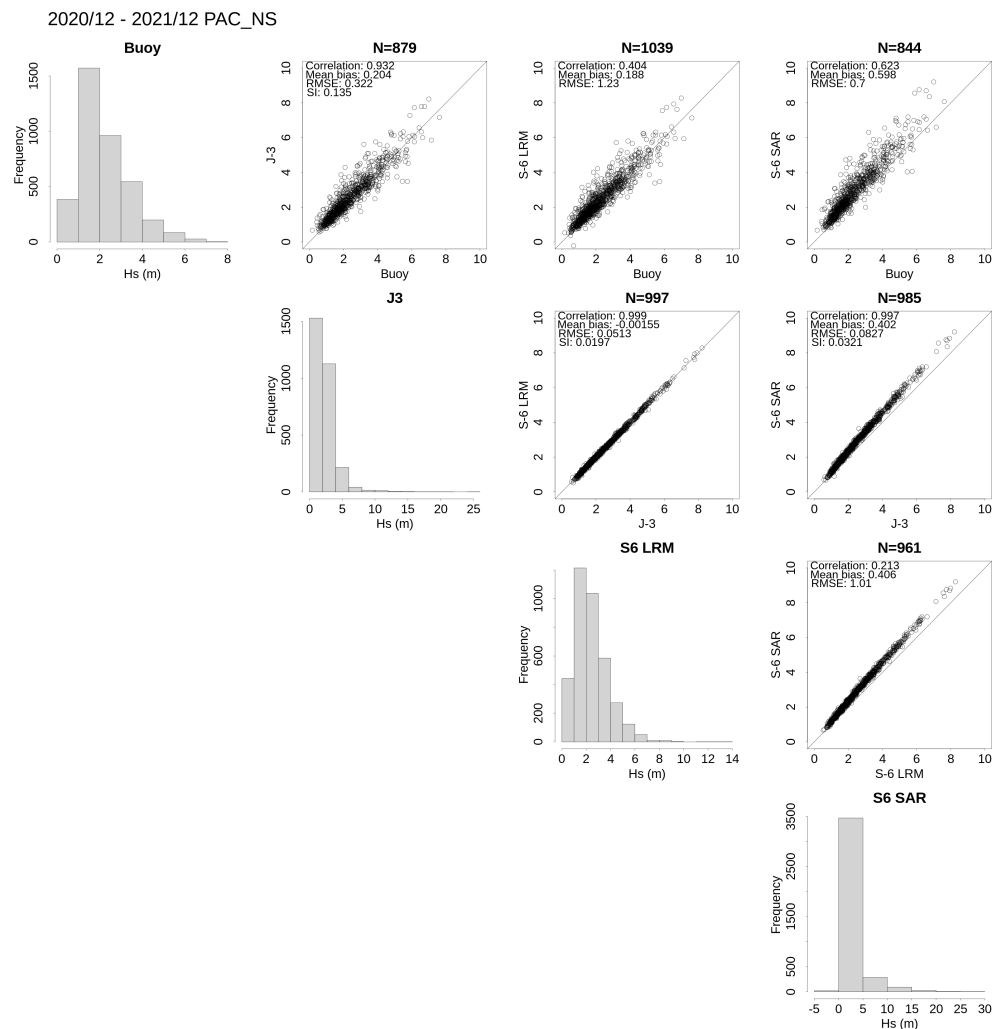


**Figure 4.** Collocations at Pacific nearshore locations with 150 km sampling.

These results can be contrasted with Figure 4 that shows similar intercomparisons with moored buoys, but in nearshore locations. The most notable difference is that RMSE is increased for all comparisons, particularly for the moored buoys. This is largely expected since the sampling radius of 150 km is likely to capture the higher spatial variability in sea state in nearshore areas. Other features, such as the excellent agreement between J3 and S6-MF LRM, and high mean bias associated with S6-MF SAR across all comparisons, are still readily apparent.

These findings motivate a closer examination of the error dependence between the altimetry datasets and, in that context, the use of a range of other varied and independent datasets for additional comparison.

### 3.2. Global error analysis

The TC method was applied first to each of the members of the tandem datasets, together with the full global *in situ* dataset and ERA5. This mitigates the issue of error dependence across the tandem data.



\*\*\* TBD

### 3.3. Regional error analysis

The TC method was applied first to each of the members of the tandem datasets, together with the full global *in situ* dataset and ERA5. This mitigates the issue of error dependence across the tandem data, such that results can be interpreted more clearly. Analysis is provided for both offshore and nearshore buoy locations. Standard deviations of the estimated error, together with their uncertainties (1 s.d.), are shown in the barplots of Figures 5 and 6.

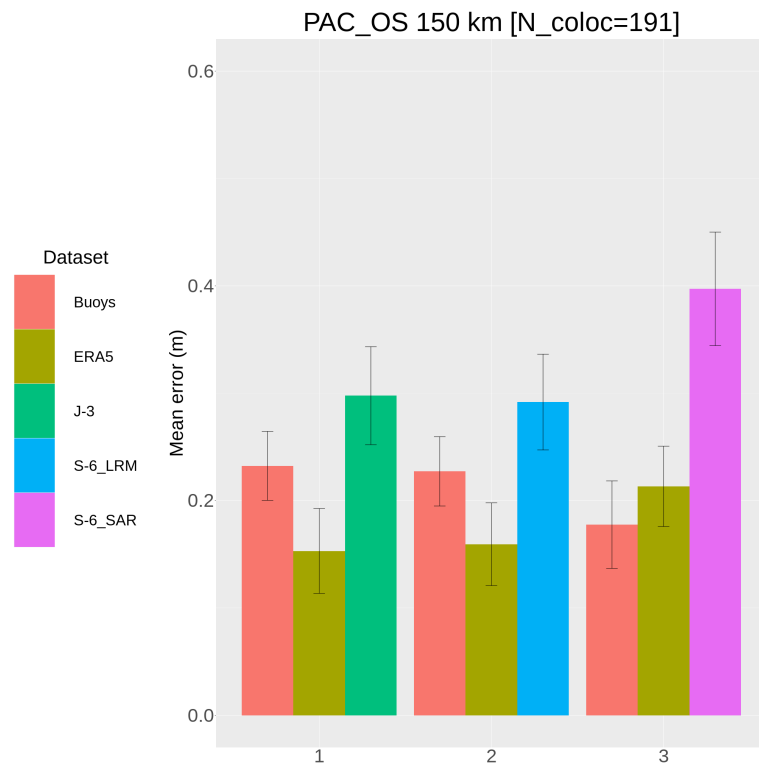


**Figure 5.** Absolute estimated mean error from three TC analyses conducted at collocations with offshore buoys in the Pacific (Figure 2). Number of collocations = 191. All groups include buoy data and ERA5. Uncertainties at 1 s.d. are shown by error bars.

Results shown in Figure 5 appear to reflect the data properties seen in Section 3.1. In particular, data groups one and two, that contain J3 and S6-LRM, show remarkable similarity, consistent with the near identical nature of the two LRM datasets. On the other hand, group 3 shows that error in S6-SAR is somewhat larger. This is linked to known variation and bias throughout the range of  $H_s$  values. Explanation of the differences in the

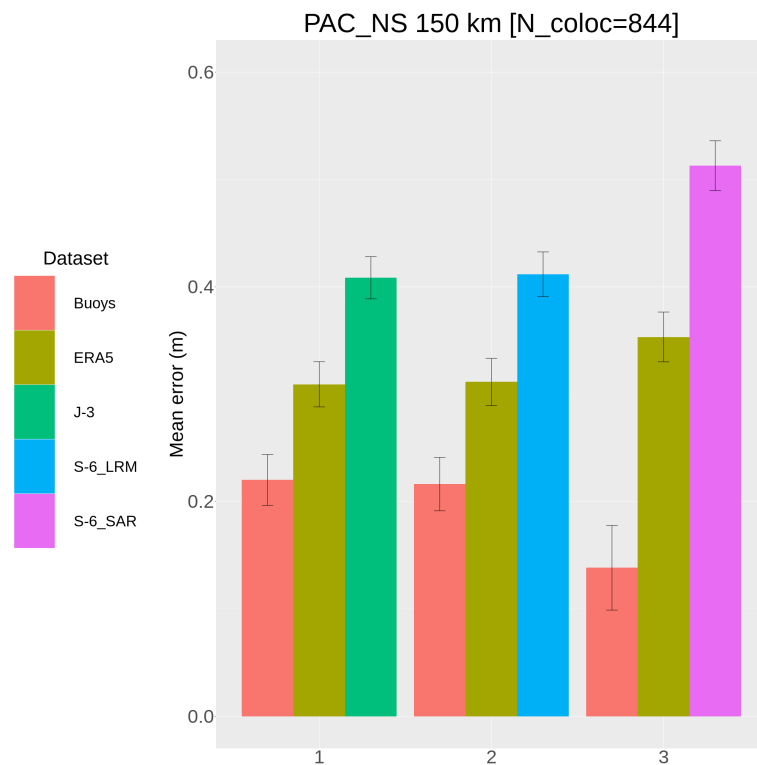


**Figure 6.** Absolute estimated mean error from three TC analyses conducted at collocations with nearshore buoys in the Pacific (Figure 2). All groups include buoy data and ERA5. Uncertainties at 1 s.d. are shown by error bars.

Reduction in the sampling radius from 150 km to 100 km results in considerable change to the respective error contributions.

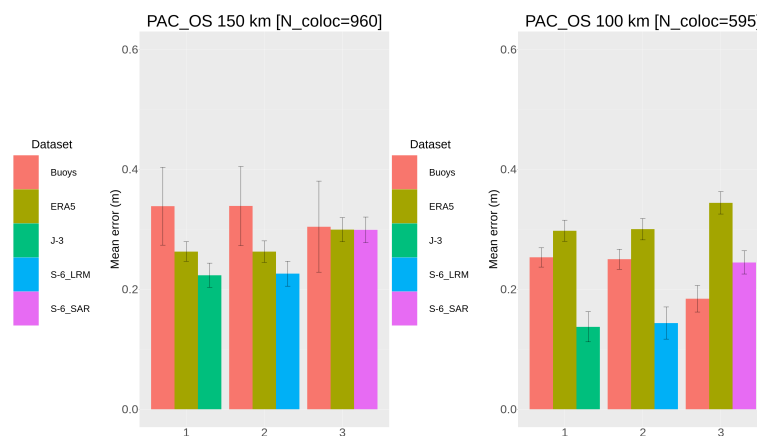


**Figure 7.** (Left side) Same as Figure 5 showing error estimates for 150 km sampling radius. (Right side) The same analysis based upon a sampling radius of 100 km.

### 3.4. Sensitivity of error analysis to sea state

Altimetry performance may be sensitive to a number of factors, including the observed sea state. S6-MF SAR observations, for example, exhibit bias and scatter throughout the range of observed  $H_s$  (see e.g. Figure 3). Empirically, we have shown that the dependence of these biases on both significant wave height and average wave period is highly significant (not shown here, maybe supplementary \*\*\*). It is important therefore to clearly understand these limitations, if they exist, for all tandem phase datasets. In order to explore whether estimated errors are a function of sea state, we use two methods to sub-sample the collocated datasets. Firstly, a basic approach based upon observed average wave period, described

in Section 3.4.1 and secondly, from specific swell partition identification described in Section 3.4.2.

### 3.4.1. Average wave period threshold

We first examine sensitivity of the analysis to sea state using a basic approach. Moored buoys typically provide continuous summary sea state parameters including average wave period ( $T_{m2}$ ). For collocations with buoys, this can be used efficiently as a means of sub-sampling to preferentially analyse more, or less, developed sea states. Here, we adopt a threshold for  $T_{m2}$  of 8 s, above which are considered to be swell dominated sea states (justification \*\*\*).

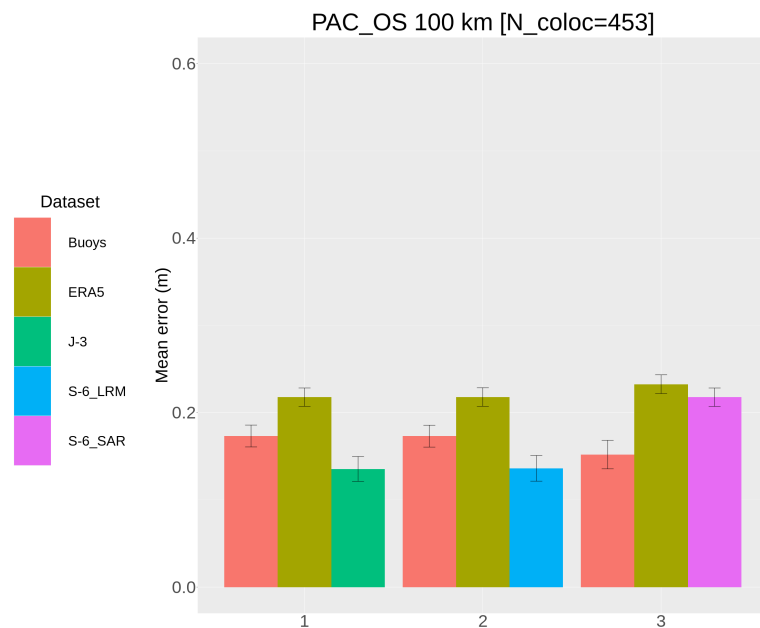


**Figure 8.** Error estimates for Pacific offshore buoy collocations using 100 km sampling radius. Only sea states corresponding to  $T_{m2} < 8$  s are used in the analysis.

For Pacific offshore buoy collocations, Figure 8 shows the absolute error estimates for sea states where  $T_{m2} < 8$  s. In terms of the relationship between the source datasets, this result is consistent with Figure 7 but exhibits systematically lower error variances. Observations from altimetry appear to compare well with moored buoys but, while the apparent uncertainties in the error estimates are quite low, the spatial scale of observations (e.g. ERA5) and quality control of all data sources, particularly the moored buoys, are likely to affect the results. Additional collocations will be advantageous. \*\*\* Further exploration needed into sensitivity to observation scale.

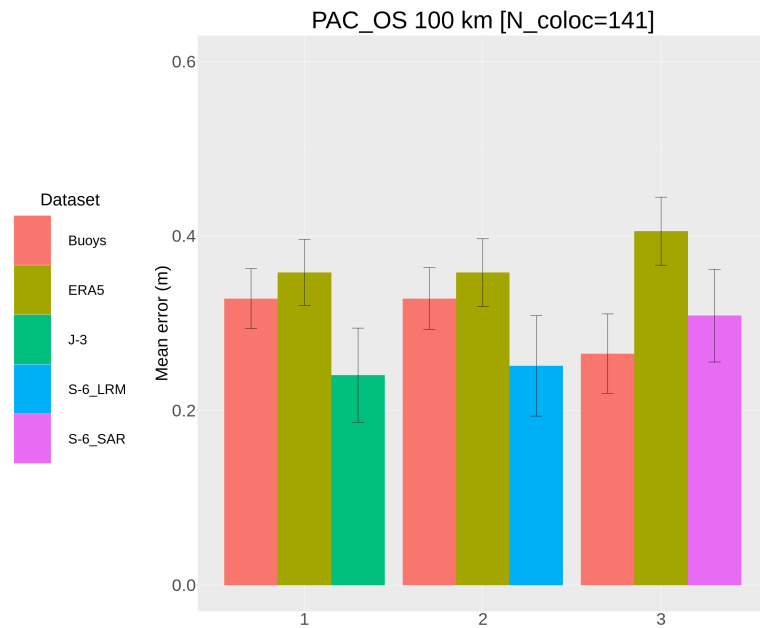


**Figure 9.** Error estimates for Pacific offshore buoy collocations using 100 km sampling radius. Only sea states corresponding to  $Tm2 > 8$  s are used in the analysis.

Contrasting the results for lower sea states with  $Tm2 > 8$  s, it is clear from Figure 11 that, again, a similar relationship is evident between the various data triplets. The obvious difference is that the error variances have increased, reflecting the larger disagreements in more energetic sea states (see also Figure 3. The smaller number of collocations results in much lower confidence in the results, and overall the same factors, linked to consistency on spatial scales and quality control are likely to be problematic. It is noticeable however that the error variance for S6-MF SAR appear to be somewhat less sensitive to sea state. \*\*\* Plots of relative error required.

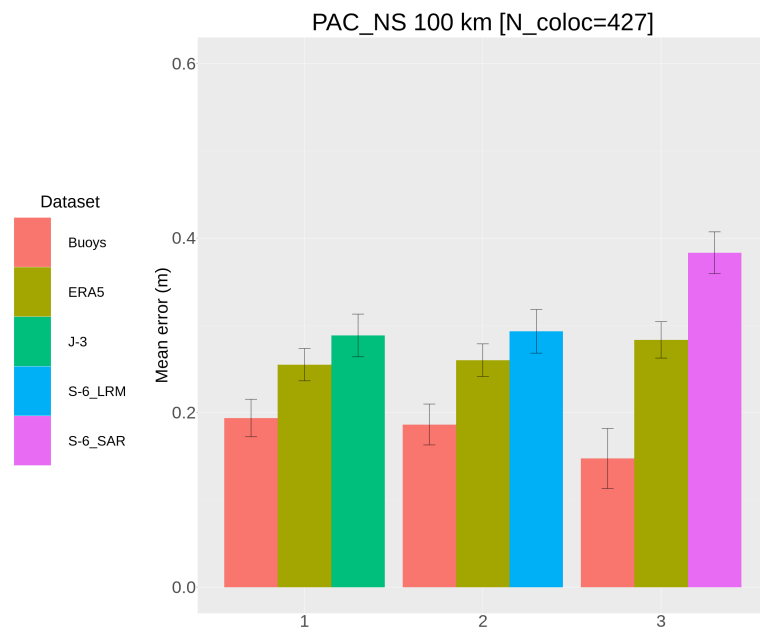


**Figure 10.** Error estimates for Pacific nearshore buoy collocations using 100 km sampling radius. Only sea states corresponding to  $Tm2 < 8$  s are used in the analysis.

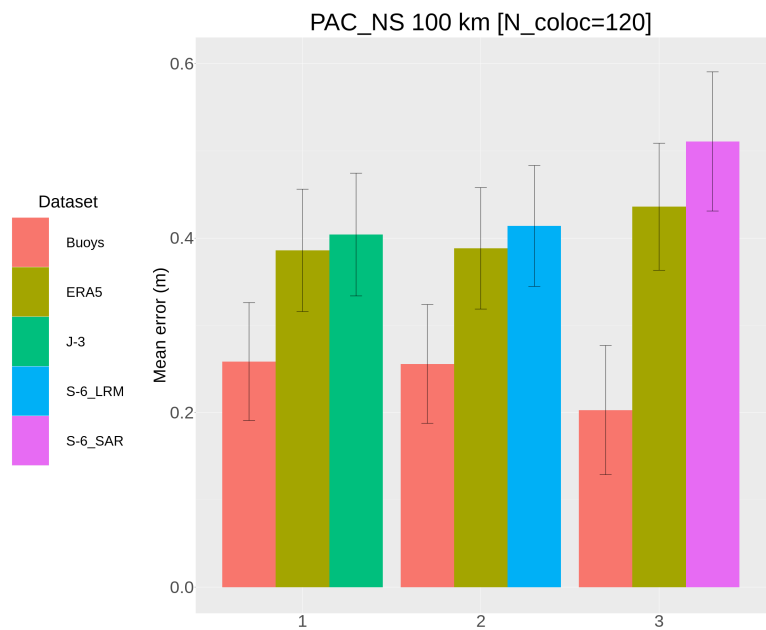


**Figure 11.** Error estimates for Pacific nearshore buoy collocations using 100 km sampling radius. Only sea states corresponding to  $Tm2 > 8$  s are used in the analysis.

Figures 10 and 11 show similar analyses w.r.t. sea state sub-sampling but for nearshore locations. Again, the overall relationship between the datasets in the three triplet groups is maintained for lower and higher energy sea states. For higher sea states ( $Tm2 > 8$  s) nearshore, although uncertainty in error estimates is fairly high (\*\* relative error plots required), it is apparent that the error variances for the moored buoys are rather lower. This is likely linked to larger sea state spatial gradients in more energetic seas which are more poorly captured in both ERA5 and by the fairly large sampling area for the altimetry observations. However, in these nearshore locations, numbers of collocations are much reduced due to quality control, which results in considerable uncertainty and a lack of statistical robustness. A larger collocation dataset will help address these issues.

3.4.2. Swell partition identification

TBD

4. Discussion

TBD

5. Conclusions

TBD

**Author Contributions:** Conceptualization, methodology and formal analysis, Timmermans, Gommenginger; data curation and production, Timmermans; writing—original draft preparation, Timmermans, Gommenginger; writing—review and editing, All authors; funding acquisition, Gommenginger. All authors have read and agreed to the published version of the manuscript.

**Funding:** This research was part-funded by the ESA S6-JTEX \*\*\*.

**Data Availability Statement:** Jason-3 data, Sentinel-6 Micheal Freilich data. Data from NDBC moored buoys is available from USACE \*\*\*. Data from CMEMS INSTAC \*\*\*. Analysis code available at [https://github.com/bwtimmermans/s6-j3\\_tandem](https://github.com/bwtimmermans/s6-j3_tandem).

**Conflicts of Interest:** The authors declare no conflict of interest.

## References

1. Meucci, A.; Young, I.R.; Aarnes, O.J.; Øyvind Breivik. Comparison of Wind Speed and Wave Height Trends from Twentieth-Century Models and Satellite Altimeters. *Journal of Climate* **2020**, *33*, 611–624. doi:10.1175/JCLI-D-19-0540.1.
2. Alday, M.; Accensi, M.; Ardhuin, F.; Dodet, G. A global wave parameter database for geophysical applications. Part 3: Improved forcing and spectral resolution. *Ocean Modelling* **2021**, *166*, 101848. doi:10.1016/j.ocemod.2021.101848.
3. Gemmrich, J.; Thomas, B.; Bouchard, R. Observational changes and trends in northeast Pacific wave records. *Geophysical Research Letters* **2011**, *38*. doi:10.1029/2011GL049518.
4. Collins, C.O.I.; Jensen, R.E. Tilt Error in NDBC Ocean Wave Height Records. *Journal of Atmospheric and Oceanic Technology* **2022**. doi:10.1175/JTECH-D-21-0079.1.
5. Dodet, G.; Piolle, J.F.; Quilfen, Y.; Abdalla, S.; Accensi, M.; Ardhuin, F.; Ash, E.; Bidlot, J.R.; Gommenginger, C.; Marechal, G.; et al. The Sea State CCI dataset v1: towards a Sea State Climate Data Record based on satellite observations. *Earth System Science Data* **2020**. doi:10.5194/essd-2019-253.
6. Passaro, M.; Hemer, M.A.; Quartly, G.D.; Schwatke, C.; Dettmering, D.; Seitz, F. Global coastal attenuation of wind-waves observed with radar altimetry. *Nature Communications* **2021**, *12*. doi:10.1038/s41467-021-23982-4.
7. Rusu, L.; Rusu, E. Evaluation of the Worldwide Wave Energy Distribution Based on ERA5 Data and Altimeter Measurements. *Energies* **2021**, *14*, 394. doi:10.3390/en14020394.
8. Marechal, G.; Ardhuin, F. Surface currents and significant wave height gradients: Matching numerical models and high-resolution altimeter wave heights in the Agulhas current region. *Journal of Geophysical Research: Oceans* **2021**, *126*. doi:10.1029/2020JC016564.
9. Timmermans, B.; Gommenginger, C.; Dodet, G.; Bidlot, J.R. Global Wave Height Trends and Variability from New Multimission Satellite Altimeter Products, Reanalyses, and Wave Buoys. *Geophysical Research Letters* **2020**, *47*, 1–11. doi:10.1029/2019GL086880.
10. Hochet, A.; Dodet, G.; Ardhuin, F.; Hemer, M.; Young, I.S. State Decadal Variability in the North Atlantic: A review. *Climate* **2021**, *9*. doi:10.3390/cli9120173.
11. Hall, C.; Jensen, R.E. USACE Coastal and Hydraulics Laboratory Quality Controlled, Consistent Measurement Archive. *Scientific Data* **2022**, *9*. doi:10.1038/s41597-022-01344-z.
12. Hersbach, H.; Bell, B.; Berrisford, P.; Hirahara, S.; Horányi, A.; Muñoz-Sabater, J.; Nicolas, J.; Peubey, C.; Radu, R.; Schepers, D.; et al. The ERA5 global reanalysis. *Quarterly Journal of the Royal Meteorological Society* **2020**, *146*, 1999–2049. doi:10.1002/qj.3803.
13. ECMWF. ERA5 data documentation. <https://confluence.ecmwf.int/display/CKB/ERA5%3A+data+documentation#heading-Observations>, accessed on 2022-08-08.
14. Jonhsen, H.; Collard, F.; R.Husson.; G.Hajduch.; A.Benchaabane.; P.Vincent. Sentinel-1 Ocean Swell Wave Spectra (OSW) Algorithm Definition. Technical Document Ref: S1-TN-NRT-52-7450 Version 1.4, 2021-12-17, Collecte Localisation Satellites.
15. Schulz-Stellenfleth, J.; König, T.; Lehner, S. An empirical approach for the retrieval of integral ocean wave parameters from synthetic aperture radar data. *Journal of Geophysical Research: Oceans* **2007**, *112*. doi:10.1029/2006JC003970.
16. Li, X.M.; Lehner, S.; Bruns, T. Ocean Wave Integral Parameter Measurements Using Envisat ASAR Wave Mode Data. *IEEE Transactions on Geoscience and Remote Sensing* **2010**, *49*. doi:10.1109/TGRS.2010.2052364.
17. Pleskachevsky, A.; Jacobsen, S.; Tings, B.; Schwarz, E. Estimation of sea state from Sentinel-1 synthetic aperture radar imagery for maritime situation awareness. *International Journal of Remote Sensing* **2019**, *40*, 4104–4142. doi:10.1080/01431161.2018.1558377.
18. Pleskachevsky, A.; Tings, B.; Wiehle, S.; Imber, J.; Jacobsen, S. Multiparametric sea state fields from synthetic aperture radar for maritime situational awareness. *Remote Sensing of Environment* **2022**, *280*. doi:10.1016/j.rse.2022.113200.
19. Tokmakian, R.; Challenor, P. On the joint estimation of model and satellite sea surface height anomaly errors. *Ocean Modelling* **1999**, *1*, 39–52.
20. Janssen, P.A.E.M.; Abdalla, S.; Hersbach, H.; Bidlot, J.R. Error Estimation of Buoy, Satellite, and Model Wave Height Data. *Journal of Atmospheric and Oceanic Technology* **2007**, *24*, 1665–1677. doi:10.1175/JTECH2069.1.
21. Wang, H.; Mouche, A.; Husson, R.; Chapron, B.; Yang, J.; Liu, J.; Ren, L. Quantifying Uncertainties in the Partitioned Swell Heights Observed From CFOSAT SWIM and Sentinel-1 SAR via Triple Collocation. *IEEE Transactions on Geoscience and Remote Sensing* **2022**, *60*. doi:10.1109/TGRS.2022.3179511.
22. Vogelzang, J.; Stoffelen, A. Triple collocation. Technical Report NWPSAF-KN-TR-021 Version 1.0, KNMI, de Bilt, the Netherlands.
23. Dodet, G.; Abdalla, S.; Alday, M.; Accensi, M.; Bidlot, J.; Ardhuin, F. Error Characterization of Significant Wave Heights in Multidecadal Satellite Altimeter Product, Model Hindcast and In Situ Measurements Using the Triple Collocation Technique. *Journal of Atmospheric and Oceanic Technology* **2022**, *39*, 887–901. doi:10.1175/JTECH-D-21-0179.1.